Luminescent Heterobimetallic Complexes. Electronic Structure and Spectroscopy of $[MPt(dppm)_2(C{\equiv}CPh)_2]PF_6$ (M = Au or Ag) and Crystal Structure of $[AuPt(dppm)_2(C{\equiv}CPh)_2]PF_6$ (dppm = $Ph_2PCH_2PPh_2$)†

Hon-Kay Yip,[a] Hsui-Mei Lin,[b] Yu Wang[b] and Chi-Ming Che*[,a,b]

[a] *Department of Chemistry, The University of Hong Kong, Pokfulam Road, Hong Kong*

[b] *Department of Chemistry, National Taiwan University, Taipei, Taiwan*

The crystal structure of $[AuPt(dppm)_2(C{\equiv}CPh)_2]PF_6{\cdot}H_2O$ (dppm = $Ph_2PCH_2PPh_2$) has been determined: triclinic, space group $P\bar{1}$, $Z = 2$, $a = 11.146(4)$, $b = 14.512(2)$, $c = 20.322(3)$ Å, $\alpha = 81.55(1)$, $\beta = 101.27(2)$, $\gamma = 109.35(2)°$. The complex cation consists of a square-planar P–Pt-$(C{\equiv}CPh)_2$–P and a linear P–Au–P moiety and the measured intramolecular Pt–Au separation is 2.910(1) Å. The absorption and emission spectra of the complex and of $[AgPt(dppm)_2(C{\equiv}CPh)_2]PF_6$ and *trans*-$[Pt(dppm)_2(C{\equiv}CPh)_2]$ have been measured. Both dinuclear complexes possess low-energy intense electronic absorption bands {$[AuPt(dppm)_2(C{\equiv}CPh)_2]PF_6$, $\lambda_{max} = 387$ nm, $\varepsilon_{max} = 1.11 \times 10^4$ dm^3 mol^{-1} cm^{-1}; $[AgPt(dppm)_2(C{\equiv}CPh)_2]PF_6$, $\lambda_{max} = 368$, $\varepsilon_{max} = 1.63 \times 10^4$ dm^3 mol^{-1} cm^{-1}} which are red-shifted from that of *trans*-$[Pt(dppm)_2(C{\equiv}CPh)_2]$. In solid form, all three complexes exhibit photoluminescence at room temperature. Extended-Hückel molecular orbital calculations have been performed on the model complexes $[AuPt(dmpm)_2(C{\equiv}CPh)_2]^+$ and *trans*-$[Pt(dmpm)_2(C{\equiv}CPh)_2]$ (dmpm = $Me_2PCH_2PMe_2$).

The spectroscopy and photochemistry of metal–acetylide complexes have attracted attention recently.[1] The intriguing photophysical and photochemical properties of platinum(II)–phenylacetylide complexes are highlighted by the photoluminescence studies on *trans*-$[Pt(PR_3)_2(C{\equiv}CPh)_2]$ (R=alkyl or Ph)[1a] and the photochemical studies on $[Pt_2(PEt_3)_4(\mu\text{-}C{=}CHPh)(C{\equiv}CPh)]$[1b] the excited state of which was found to react with methyl iodide, propan-2-ol and diphenylacetylene.

In the course of our study on luminescent heterobimetallic d^{10}–d^8 complexes[2] we investigated $[MPt(dppm)_2(C{\equiv}CPh)_2]^+$ (M = Au or Ag, dppm = $Ph_2PCH_2PPh_2$) which were synthesised by Shaw and co-workers.[3] Their spectroscopic properties were found to be interesting, being different from those of $[MPt(dppm)_2(CN)_2]^+$.[2]

Experimental

Materials.—The ligand dppm (Aldrich, 98%), $K[AuCl_4]$ (Aldrich, 98%), PPh_3 (Merck, 98%), $K_2[PtCl_4]$ (Aldrich, 99%), $AgPF_6$ (BDH, LR), phenylacetylene (Aldrich, 98%), and $Hg(O_2CMe)_2$ (BDH, 98%) were used as received.

Syntheses.—The complexes *trans*-$[Pt(dppm)_2(C{\equiv}CPh)_2]$[3a] and $[MPt(dppm)_2(C{\equiv}CPh)_2]PF_6$ (M = Au or Ag)[3b] were synthesised by the methods reported by Shaw and co-workers.

Instrumentation.—The UV/VIS absorption spectra were recorded on a Milton Roy Spectronic 3000 diode-array spectrophotometer, room-temperature and 77 K solid-state and glass emission spectra on a Spex Fluorolog-2 spectrofluorometer, infrared spectra as Nujol mulls on a Nicolet 20SX FT-IR spectrometer and ^{1}H NMR spectra on a JEOL GSX 270 MHz spectrometer with $SiMe_4$ used as standard. Emission lifetimes were recorded with the laser photolysis set-up described elsewhere.[4]

Molecular Orbital Calculations.—Extended-Hückel molecular orbital (EHMO) calculations were made on $[AuPt(dmpm)_2(C{\equiv}CPh)_2]^+$ and *trans*-$[Pt(dmpm)_2)(C{\equiv}CPh)_2]$ (dmpm = $Me_2PCH_2PMe_2$). The geometry of the former species was taken from X-ray diffraction data with all phenyl groups on P replaced by methyl groups. The geometry of the latter is the same as the former with the Au atom removed. The calculations were carried out using the ICON program[5] and the H_{ii} and ξ values for Au and Pt were taken from the literature.[6]

Crystal Structure Determination of $[AuPt(dppm)_2(C{\equiv}CPh)_2]PF_6{\cdot}H_2O$.—A suitable crystal of $[AuPt(dppm)_2(C{\equiv}CPh)_2]PF_6{\cdot}H_2O$ (dimensions 0.50 × 0.60 × 0.60 mm) was chosen for X-ray analysis.

Crystal data. $C_{66}H_{54}AuF_6OP_5Pt$, $M = 1524.05$, triclinic, space group $P\bar{1}$, $a = 11.146(4)$, $b = 14.512(2)$, $c = 20.322(3)$ Å, $\alpha = 81.55(1)$, $\beta = 101.27(2)$, $\gamma = 109.35(2)°$, $D_c = 1.65$ g cm^{-3}, $U = 3030(1)$ Å^3, $Z = 2$, μ(Mo-Kα) = 48.7 cm^{-1}, $F(000) = 3048$.

Intensity data were measured on a CAD-4 diffractometer with Mo-Kα ($\lambda = 0.7093$ Å) radiation using a θ–2θ scan technique. A total of 7884 unique reflections was measured, of which 6265 were observed [$I \geqslant 2\sigma(I)$] and were based on the least-squares refinement. Intensities were corrected for absorption based on experimental ψ curves for three chosen reflections. Three standard reflections were monitored throughout the intensity measurement, but their intensity variations were less than ±2%. During the least-squares refinement all the phenyl ring groups were considered to be rigid, *i.e.* all the C–C bonds were fixed at 1.395 Å, C–H at 1.0 Å, and C–C–C angles at 120°. For each, anisotropic group thermal motion plus individual atomic isotropic thermal motion were considered. A secondary isotropic extinction correction was applied, $1.19(4) \times 10^{-4}$. One water molecule of solvation is

† *Supplementary data available:* see Instructions for Authors, *J. Chem. Soc., Dalton Trans.*, 1993, Issue 1, pp. xxiii–xxviii.

Non-SI unit employed: eV ≈ 1.60×10^{-19} J.

Table 1 Atomic coordinates of $[AuPt(dppm)_2(C{\equiv}CPh)_2]PF_6{\cdot}H_2O$

Atom	x	y	z	Atom	x	y	z
Au	0.443 12(5)	0.222 59(3)	0.300 16(3)	C(13B)	0.838 7(10)	0.508 4(6)	0.472 2(6)
Pt	0.566 62(5)	0.175 91(3)	0.201 52(3)	C(14B)	0.830 1(11)	0.431 4(10)	0.522 8(4)
P(1)	0.589 1(3)	0.378 37(22)	0.313 23(17)	C(15B)	0.748 5(13)	0.337 5(8)	0.509 7(5)
P(2)	0.649 4(3)	0.343 84(21)	0.181 56(16)	C(16B)	0.675 4(10)	0.320 6(5)	0.446 1(6)
P(3)	0.281 1(3)	0.074 28(22)	0.287 95(17)	C(21A)	0.544 0(7)	0.410 9(6)	0.135 7(4)
P(4)	0.472 0(3)	0.010 47(21)	0.224 81(16)	C(22A)	0.413 7(8)	0.375 9(4)	0.141 9(4)
C(1)	0.710 9(10)	0.404 3(7)	0.259 6(5)	C(23A)	0.332 8(6)	0.431 4(7)	0.112 6(5)
C(2)	0.306 1(10)	−0.009 1(8)	0.236 1(6)	C(24A)	0.382 2(9)	0.521 9(6)	0.077 0(4)
C(3)	0.713 7(10)	0.187 2(7)	0.274 1(6)	C(25A)	0.512 4(10)	0.556 9(5)	0.070 8(4)
C(4)	0.813 3(11)	0.199 6(8)	0.315 4(6)	C(26A)	0.593 3(6)	0.501 4(6)	0.100 1(5)
C(5)	0.426 3(11)	0.168 1(7)	0.125 8(6)	C(21B)	0.784 9(7)	0.374 1(6)	0.137 2(4)
C(6)	0.335 4(12)	0.165 6(8)	0.079 9(6)	C(22B)	0.901 9(9)	0.446 4(6)	0.154 5(3)
P	0.033 8(4)	0.678 4(3)	0.274 58(19)	C(23B)	1.001 4(6)	0.464 7(5)	0.117 3(5)
F(1)	−0.105 0(7)	0.639 5(5)	0.232 6(4)	C(24B)	0.984 0(7)	0.410 8(7)	0.062 8(4)
F(2)	0.174 5(8)	0.718 6(6)	0.314 5(4)	C(25B)	0.867 1(9)	0.338 5(6)	0.045 5(3)
F(3)	0.026 1(9)	0.571 8(5)	0.304 9(4)	C(26B)	0.767 5(6)	0.320 1(5)	0.082 7(4)
F(4)	0.045 0(8)	0.785 8(5)	0.242 6(4)	C(31A)	0.131 9(6)	0.091 7(6)	0.245 1(4)
F(5)	0.092 3(8)	0.662 5(6)	0.213 0(4)	C(32A)	0.033 8(8)	0.015 7(4)	0.213 9(4)
F(6)	−0.022 8(9)	0.693 3(6)	0.335 7(4)	C(33A)	−0.078 5(7)	0.032 6(5)	0.178 4(4)
O	0.521(3)	0.585 0(16)	0.486 0(15)	C(34A)	−0.092 8(7)	0.125 3(7)	0.174 0(4)
C(11)	0.934 5(6)	0.212 7(8)	0.359 7(4)	C(35A)	0.005 3(10)	0.201 2(5)	0.205 2(5)
C(12)	1.016 6(9)	0.306 9(6)	0.371 5(4)	C(36A)	0.117 6(8)	0.184 4(5)	0.240 7(4)
C(13)	1.137 3(8)	0.319 7(5)	0.411 1(5)	C(31B)	0.256 3(9)	0.007 1(6)	0.369 3(3)
C(14)	1.175 9(7)	0.238 2(8)	0.438 8(4)	C(32B)	0.348 4(7)	0.037 9(5)	0.425 6(5)
C(15)	1.093 7(10)	0.144 0(6)	0.427 0(5)	C(33B)	0.332 4(9)	−0.012 9(7)	0.488 7(4)
C(16)	0.973 0(9)	0.131 3(5)	0.387 4(5)	C(34B)	0.224 2(11)	−0.094 5(7)	0.495 6(4)
C(21)	0.225 7(10)	0.169 6(10)	0.029 3(6)	C(35B)	0.132 1(8)	−0.125 3(5)	0.439 4(6)
C(22)	0.102 2(14)	0.129 8(9)	0.046 2(4)	C(36B)	0.148 2(8)	−0.074 5(7)	0.376 3(4)
C(23)	−0.004 3(9)	0.136 9(10)	−0.001 0(7)	C(41A)	0.545 1(8)	−0.056 2(5)	0.294 1(4)
C(24)	0.012 8(12)	0.183 9(10)	−0.065 1(6)	C(42A)	0.671 4(8)	−0.052 6(5)	0.293 1(4)
C(25)	0.136 3(16)	0.223 7(10)	−0.081 9(5)	C(43A)	0.728 5(7)	−0.112 1(7)	0.339 9(5)
C(26)	0.242 8(10)	0.216 6(10)	−0.034 7(8)	C(44A)	0.659 4(11)	−0.175 4(6)	0.387 8(4)
C(11A)	0.511 4(8)	0.472 8(5)	0.292 7(4)	C(45A)	0.533 1(11)	−0.179 0(6)	0.388 9(4)
C(12A)	0.384 7(8)	0.448 6(5)	0.304 1(4)	C(46A)	0.476 0(7)	−0.119 5(7)	0.342 0(5)
C(13A)	0.322 6(7)	0.520 0(7)	0.292 1(5)	C(41B)	0.453 6(8)	−0.062 4(5)	0.156 4(3)
C(14A)	0.387 2(9)	0.615 5(6)	0.268 7(5)	C(42B)	0.535 6(7)	−0.026 6(5)	0.108 3(5)
C(15A)	0.513 9(9)	0.639 7(4)	0.257 3(5)	C(43B)	0.532 4(9)	−0.086 2(8)	0.059 6(4)
C(16A)	0.576 0(6)	0.568 3(6)	0.269 3(5)	C(44B)	0.447 2(11)	−0.181 5(7)	0.059 0(4)
C(11B)	0.684 0(10)	0.397 6(8)	0.395 5(4)	C(45B)	0.365 2(9)	−0.217 3(4)	0.107 1(5)
C(12B)	0.765 6(12)	0.491 5(6)	0.408 5(5)	C(46B)	0.368 4(7)	−0.157 7(6)	0.155 8(4)

Table 2 Selected bond distances (Å) and angles (°) of $[AuPt(dppm)_2(C{\equiv}CPh)_2]PF_6{\cdot}H_2O$

Au–Pt	2.910(1)	Pt–C(3)	1.958(11)
Au–P(1)	2.323(3)	Pt–C(5)	1.954(11)
Au–P(3)	2.315(3)	C(3)–C(4)	1.23(2)
Pt–P(2)	2.307(3)	C(5)–C(6)	1.23(2)
Pt–P(4)	2.299(3)	C(4)–C(11)	1.44(1)
P(1)–Au–P(3)	174.0(1)	C(3)–Pt–C(5)	177.0(4)
P(2)–Pt–P(4)	175.7(1)	Pt–C(3)–C(4)	174.0(9)
P(2)–Pt–C(3)	85.9(3)	Pt–C(5)–C(6)	177(1)
P(2)–Pt–C(5)	92.4(3)	C(3)–C(4)–C(11)	176(1)

present in the crystal. All the crystallographic computations were made on a Micro VAX computer using the NRCVAX program.[7] Convergence of 6265 observed data and 717 parameters was reached at $R = 0.044$, $R' = 0.039$ and $S = 3.90$ with weighting scheme $w = [\sigma^2(F_o)]^{-1}$. The final Fourier difference map showed residual extrema in the range +1.59 to −1.27 e Å^{-3}. Atomic coordinates for non-hydrogen atoms are listed in Table 1, bond distances and angles in Table 2.

Additional material available from the Cambridge Crystallographic Data Centre comprises H-atom coordinates, thermal parameters and remaining bond lengths and angles.

Results and Discussion

The synthesis and characterization of the d^{10}–d^8 heterobimetallic complexes $[MPt(dppm)_2(C{\equiv}CPh)_2]^+$ (M = Ag, Cu, Au or $HgCl_2$) were previously reported by Shaw and coworkers.[3] This work presents the first spectroscopic investigation of the complexes.

Fig. 1 shows a perspective view of the $[AuPt(dppm)_2(C{\equiv}CPh_2)]^+$ cation. The structure is similar to that of $[AuPt(dppm)_2(CN)_2]^+$, having a pseudo-square-planar $Pt(C{\equiv}CPh)_2P_2$ unit and a closely linear P–Au–P moiety bridged by two *trans*-dppm ligands. The intramolecular Pt–Au distance is 2.910(1) Å which is shorter than the value of 3.046(2) Å in $[AuPt(dppm)_2(CN)_2]^+$ (ref. 2) and the Pt–Ag distance of 3.146(3) Å in $[AgPt(dppm)_2(C{\equiv}CPh)_2I]$.[8] While the other bond distances in $[AuPt(dppm)_2(C{\equiv}CPh)_2]^+$ and $[AuPt(dppm)_2(CN)_2]^+$ are normal, the short Pt–Au separation may have an electronic origin.

Electronic Spectroscopy of $[MPt(dppm)_2(C{\equiv}CPh)_2]PF_6$ (M = Au *or* Ag).—It is rewarding to examine first the absorption spectrum of *trans*-$[Pt(dppm)_2(C{\equiv}CPh)_2]$. Fig. 2 shows the spectrum measured in acetonitrile at room temperature. It exhibits an intense absorption band at 345 nm ($\varepsilon_{max} = 9.24 \times 10^3$ dm^3 mol^{-1} cm^{-1}), which is unsymmetric and is overlapped by a moderately intense absorption ($\varepsilon \approx 700$–2000 dm^3 mol^{-1} cm^{-1}) between 365 and 420 nm. Apart from these bands, there is also an intense band at 259 nm ($\varepsilon_{max} = 2.10 \times 10^4$ dm^3 mol^{-1} cm^{-1}) accompanied by a shoulder at about 293 nm ($\varepsilon \approx 1 \times 10^4$ dm^3 mol^{-1} cm^{-1}).

The electronic structure and absorption spectra of the related complexes *trans*-$[Pt(PR_3)_2(C{\equiv}CPh)_2]$ (R = alkyl, H or Ph) were examined by Masai *et al.*[9] before and recently Demas

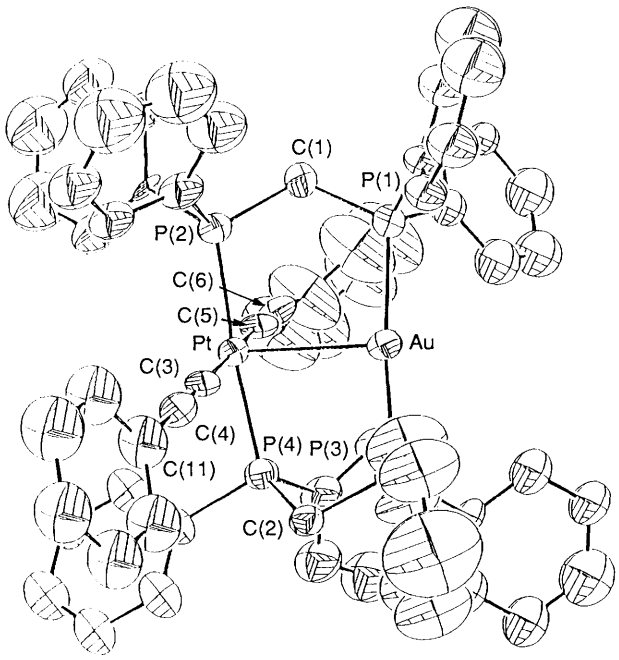

Fig. 1 Perspective view of $[AuPt(dppm)_2(C{\equiv}CPh)_2]^+$

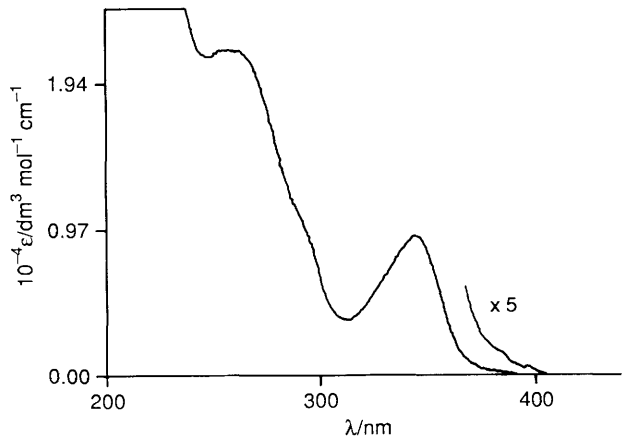

Fig. 2 The UV/VIS absorption spectrum of *trans*-$[Pt(dppm)_2(C{\equiv}CPh)_2]$ in acetonitrile solution

and co-workers [1a] reported the absorption and emission spectra of similar complexes. The absorption spectrum of *trans*-$[Pt(PEt_3)_2(C{\equiv}CPh)_2]$ shows bands at 328, 288 and 264 nm,[9] similar to those of *trans*-$[Pt(dppm)_2(C{\equiv}CPh)_2]$ studied in this work. The band of 328 nm of *trans*-$[Pt(PEt_3)_2(C{\equiv}CPh)_2]$ has been assigned to the ^{1}m.l.c.t. (metal to ligand charge transfer) transition Pt(5d)→C≡CPh.[9] It seems that the band of *trans*-$[Pt(dppm)_2(C{\equiv}CPh)_2]$ at 345 nm may be due to a similar transition. However, the ε_{max} values of these two bands are much larger than those of ^{1}m.l.c.t. transitions of square-planar platinum(II)–α-diimine complexes such as $[Pt(bipy)Cl_2]$ (bipy = 2,2′-bipyridine; λ_{max} = 394 nm, ε_{max} = 3.29 × 10^3 dm^3 mol^{-1} cm^{-1} in butyronitrile)[10] and the corresponding 3,3′-dicarboxy derivative (λ_{max} = 444 nm, ε_{max} = 3.03 × 10^3 dm^3 mol^{-1} cm^{-1} in CH_2Cl_2).[11]

Extended-Hückel molecular orbital calculations were performed on the model complex *trans*-$[Pt(dmpm)_2(C{\equiv}CPh)_2]$. The axes were chosen such that the phenylacetylides are lying along the *y* axis and the P–Pt–P vector is designated as the *x* axis. The results show that there is substantial mixing of the π* orbital of phenylacetylide with the $6p_z$ orbital of Pt (see 1π* orbital in Fig. 3) and of the $5d_{yz}$ orbital of Pt with π orbitals of the phenylacetylide (see 1π orbital in Fig. 3). This is consistent with the calculations performed by Masai *et al.*[9] on *trans*-$[Pt(PEt_3)_2(C{\equiv}CPh)_2]$ in that π-bond interaction between the $5d_{yz}$ orbital of Pt and π orbitals of the phenylacetylide would lead to an antibonding orbital having both platinum and phenylacetylide character. Thus the band of *trans*-$[Pt(dppm)_2(C{\equiv}CPh)_2]$ at 345 nm is assigned to the spin-allowed 1π ⟶ 1π* transition, which may also be regarded as a hybrid of the conventional m.l.c.t. [Pt(5d)→C≡CPh] and intraligand π ⟶ π* transitions. Its large ε_{max} value may be accounted for by the mixing of the Pt(5d) orbitals with the π orbitals of phenylacetylide.

Upon photoexcitation, *trans*-$[Pt(dppm)_2(C{\equiv}CPh)_2]$ exhibits intense emission in the solid state but no emission was detected in fluid solution at room temperature. Fig. 4 shows the emission spectrum of the complex upon excitation at 350 nm in a MeOH–EtOH (1:4, v/v) glass at 77 K. The spectrum is rich in vibronic structure and very similar to that of *trans*-$[Pt(PEt_3)_2(C{\equiv}CPh)_2]$ reported by Demas and co-workers.[1a] The solid-state emission lifetime is 0.3 μs measured at room temperature. The vibrational progressions of 2065 and 2126 cm^{-1} (Fig. 4) compare favourably with the ground state ν(C≡C) stretch (2105 cm^{-1}) of *trans*-$[Pt(dppm)_2(C{\equiv}CPh)_2]$. The Huang–Rhys factor[12] of the progression, defined as I(01)(448 nm)/I(00)(493 nm), is estimated to be 0.3. The spectrum also exhibits another vibronic progression of ≈650 cm^{-1} and this is assigned to the phenyl-ring skeletal vibration (620–639 cm^{-1}).

The absorption spectrum of $[AuPt(dppm)_2(C{\equiv}CPh)_2]^+$ is significantly different from that of *trans*-$[Pt(dppm)_2(C{\equiv}CPh)_2]$. As shown in Fig. 5, $[AuPt(dppm)_2(C{\equiv}CPh)_2]^+$ shows an intense absorption band (A) at 387 nm (ε_{max} = 1.11 × 10^4 dm^3 mol^{-1} cm^{-1}) and an unsymmetric absorption at 329 nm (band B, ε_{max} = 1.64 × 10^4 dm^3 mol^{-1} cm^{-1}). From previous spectroscopic studies of dinuclear d^8–d^8 (ref. 13), d^{10}–d^{10} (ref. 14) and d^8–d^{10} (refs. 2 and 15) complexes, the distinct difference between the absorption spectra of dinuclear complexes and their mononuclear counterparts is the appearance of a $^1(d_{\sigma^*} \longrightarrow p_\sigma)$ transition, which is red-shifted from the absorption spectrum of the mononuclear metal complexes.

Although assigning band A to the conventional $^1(d_{\sigma^*} \longrightarrow p_\sigma)$ transition seems to be appealing, the difference between $[AuPt(dppm)_2(C{\equiv}CPh)_2]^+$ and a conventional dinuclear d^8–d^8 complex such as $[Pt_2(H_2P_2O_5)_4]^{4-}$ [ref. 13(*a*)] should not be overlooked. The result of the EHMO calculation on the electronic structure of the model complex $[AuPt(dmpm)_2(C{\equiv}CPh)_2]^+$ is shown in Fig. 6. The lowest unoccupied molecular orbital (LUMO) (also labelled as 1π*) is almost the same as that of *trans*-$[Pt(dmpm)_2(C{\equiv}CPh)_2]$. However, the previous $5d_{z^2}$ orbital of *trans*-$[Pt(dmpm)_2(C{\equiv}CPh)_2]$ changes to the d_{σ^*} orbital which is composed of significant portions of metal-localized $5d_{z^2}$ orbitals of Au and Pt. Thus, the band of $[AuPt(dmpm)_2(C{\equiv}CPh)_2]^+$ at 387 nm, which is red-shifted from that of *trans*-$[Pt(dppm)_2(C{\equiv}CPh)_2]$, is tentatively assigned to $^1(d_{\sigma^*} \longrightarrow 1\pi^*)$. However, it can also be regarded as a m.m.l.c.t. (metal–metal bond-to-ligand charge transfer) transition since the 1π* orbital here mainly arises from the phenylacetylide. The notion of a m.m.l.c.t. transition was first devised by Balch[16] in 1976 to assign the lowest-energy transition of several dinuclear rhodium(I) complexes, $[Rh_2(dppm)_2(CNR)_4]^{2+}$ (R = aryl or alkyl). However, it remains to be explained why the $^1(d_{\sigma^*} \longrightarrow 1\pi^*)$ transition is the lowest energy allowed transition in $[AuPt(dppm)_2(C{\equiv}CPh)_2]^+$ despite the fact that the Pt–Au(d_{σ^*}) orbital is not the highest occupied molecular orbital in the EHMO calculation.

The $[AuPt(dppm)_2(C{\equiv}CPh)_2]^+$ complex also exhibits two poorly resolved absorption peaks at 329 and ≈352 nm which are close in energy to the band of *trans*-$[Pt(dppm)_2(C{\equiv}CPh)_2]$ at 345 nm. Accordingly we assign these to the 1π ⟶ 1π* transition (where 1π is a hybrid of the $5d_{xz}$ of Pt and π orbital of phenylacetylide). This assignment is further supported by a similar band in the spectrum of $[AgPt(dppm)_2(C{\equiv}CPh)_2]^+$.

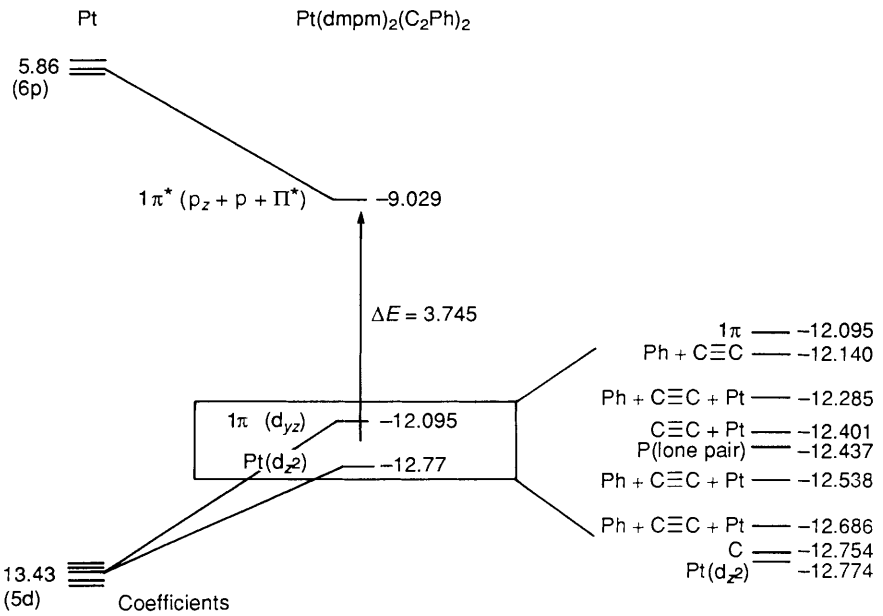

Coefficients

d_{z^2}	1π	1π*
Pt d_{z^2} 0.44153	Pt d_{yz} 0.31234	Pt p_z 0.29476
P(1)p_x −0.41 P(3)p_x 0.32 with P(1), P(3) lone pair	C(3) p_z −0.16 } π_{3-4} C(4) p_z −0.17 C(5) p_z 0.26 } π_{5-6} C(6) p_z 0.21	C(3) p_z 0.33 } π^*_{3-4} C(4) p_z −0.32 C(5) p_z 0.14 } π^*_{5-6} C(6) p_z −0.24
		P(2) p_z 0.13 p_{xz} 0.23 P(4) p_z 0.15 p_{xz} −0.21

Fig. 3 Molecular orbital diagram of *trans*-[Pt(dmpm)$_2$(C≡CPh)$_2$]; energies in eV

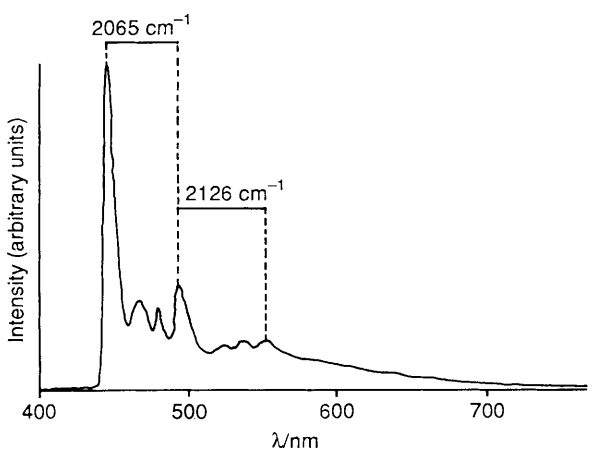

Fig. 4 Emission spectrum at 77 K of MeOH–EtOH (1:4, v/v) glass solution of *trans*-[Pt(dppm)$_2$(C≡CPh)$_2$]

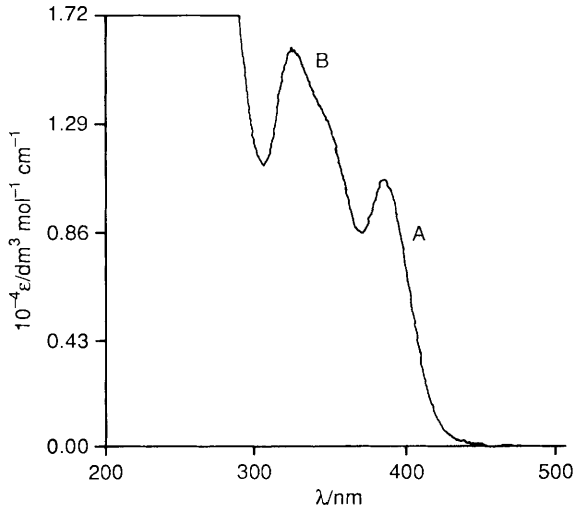

Fig. 5 The UV/VIS absorption spectrum of [AuPt(dppm)$_2$(C≡CPh)$_2$]PF$_6$ in acetonitrile solution

The solid form of [AuPt(dppm)$_2$(C≡CPh)$_2$]PF$_6$ is strongly emissive upon photoexcitation. However no emission was observed in fluid solution at room temperature. Fig. 7 shows the emission spectrum (excitation at 350 nm) of the complex in a MeOH–EtOH (1:4, v/v) glass at 77 K. The room-temperature emission spectrum shows an unsymmetric and narrow band at 462 nm and there is a shoulder at about 510 nm. The decay of the emission is monoexponential with a lifetime of 0.35 μs. At 77 K the emission intensity is increased and the band width reduced. The emission maximum is blue-shifted slightly to 454 nm and a rather distinct shoulder appears at 502 nm. It is likely that the emission becomes vibronically structured with a spacing of 2106 cm^{-1} which is nearly the same as the ground-state ν(C≡C) stretch (2105 cm^{-1}) of *trans*-[Pt(dppm)$_2$(C≡CPh)$_2$]. The Huang–Rhys factor,[12] $I(01)/I(00)$, of the emission is estimated to be about 0.2. The excitation spectrum for the 450 nm emission of [AuPt(dppm)$_2$(C≡CPh)$_2$]$^+$ at 77 K exhibits two distinct bands at 320–350 and 390 nm which have been assigned to the $^1(1\pi \longrightarrow 1\pi^*)$ and $^1(d_{\sigma^*} \longrightarrow 1\pi^*)$ transitions, respectively (Fig. 7).

The UV/VIS absorption spectrum of [AgPt(dppm)$_2$(C≡CPh)$_2$]PF$_6$ is displayed in Fig. 8. It is similar to that of its

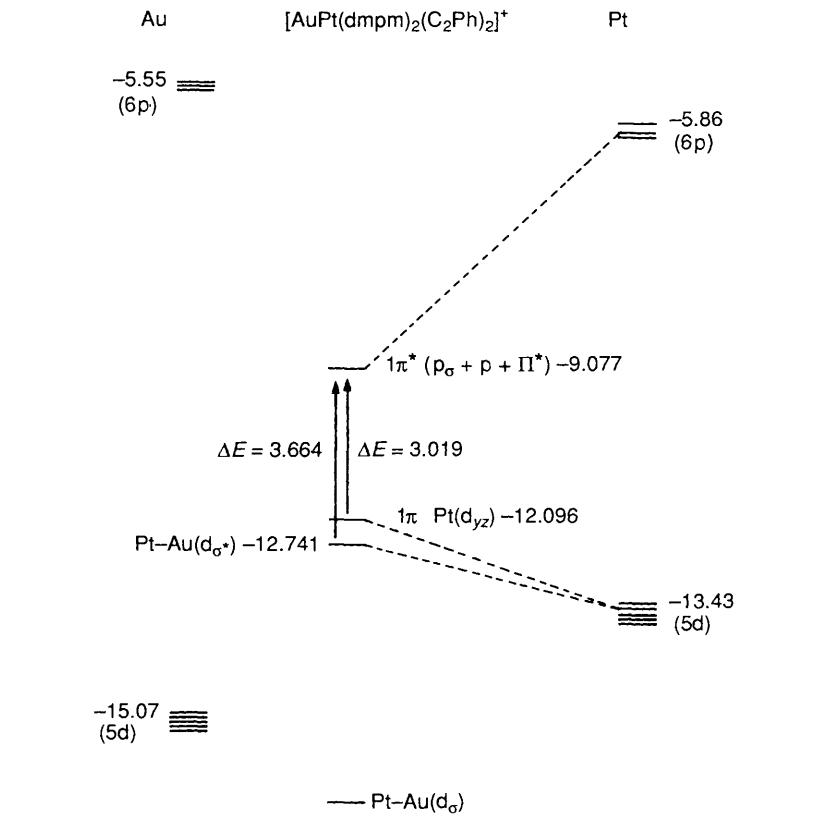

Coefficients

Pt–Au (d_{σ^*})				Pt(d_{yz})1π				1π*			
Au	d_{z^2} −0.234	} σ*	d_{xy} −0.126	Au				Au	p_z 0.160	} σ	
			s −0.149	Pt	d_{yz} 0.311			Pt	p_z −0.261		
Pt	d_{z^2} 0.660		d_{xy} −0.110	C(3)	p_z −0.157	} π		C(3)	p_z −0.288	} π*	
			s 0.188	C(4)	p_z −0.172			C(4)	p_z 0.293		
C(5)	p_x −0.159	} π		C(5)	p_z 0.260	} π		C(5)	p_z −0.123	} π*	
C(6)	p_x −0.196			C(6)	p_z 0.210			C(6)	p_z 0.221		
P(3)	p_x 0.118	} σ						P	d_{xz}		
P(4)	p_x −0.145										

Fig. 6 Molecular orbital diagram of $[AuPt(dmpm)_2(C{\equiv}CPh)_2]^+$; energies in eV

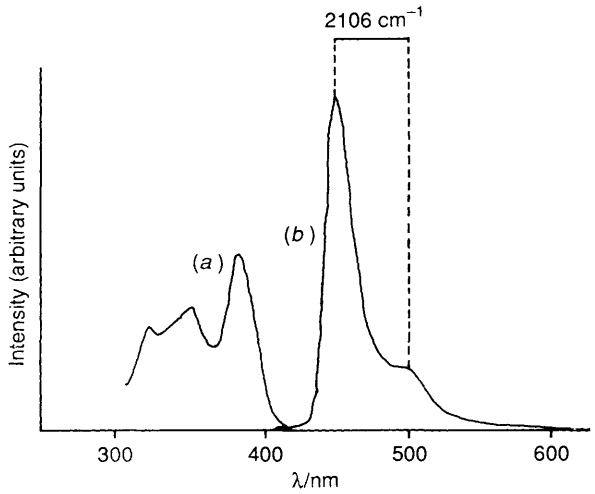

Fig. 7 Excitation (*a*) and emission (*b*) spectra at 77 K of a MeOH–EtOH (1:4, v/v) glass solution of $[AuPt(dppm)_2(C{\equiv}CPh)_2]PF_6$

gold(I) analogue. Two intense bands at 368 (ε_{max} = 1.63 × 10^4 dm^3 mol^{-1} cm^{-1}) and 318 nm (ε_{max} = 1.71 × 10^4 dm^3 mol^{-1} cm^{-1}), which could be related to the respective bands A [$^1(d_{\sigma^*} \longrightarrow 1\pi^*)$] and B [$^1(1\pi \longrightarrow 1\pi^*)$] of $[AuPt(dppm)_2(C{\equiv}CPh)_2]^+$, are evident. The $^1(d_{\sigma^*} \longrightarrow 1\pi^*)$ transition found in $[AgPt(dppm)_2(C{\equiv}CPh)_2]^+$ is higher in energy than that of the gold(I) analogue (difference ≈1470 cm^{-1}) and this is consistent with the X-ray data that the Pt–Ag interaction in $[AgPt(dppm)_2(C{\equiv}CPh)_2I]$ is weaker than the Pt–Au interaction in $[AuPt(dppm)_2(C{\equiv}CPh)_2]^+$.

Solid $[AgPt(dppm)_2(C{\equiv}CPh)_2]PF_6$ also gives a bright green emission upon photoexcitation. At room temperature the emission maximum is at 495 nm with a lifetime of 0.2 μs. The emission spectrum at 77 K of a MeOH–EtOH (1:4, v/v) glass solution of the complex is shown in Fig. 8. The emission maximum is blue-shifted to 449 nm and the band width is reduced. The emission-band profile of $[AgPt(dppm)_2(C{\equiv}CPh)_2]^+$ is different from those of $[AuPt(dppm)_2(C{\equiv}CPh)_2]^+$ and *trans*-$[Pt(dppm)_2(C{\equiv}CPh)_2]$. In the emission spectrum of $[AgPt(dppm)_2(C{\equiv}CPh)_2]^+$ two vibronic progressions can be roughly assigned: the 0–0 transition at 435 nm and the 0–1 transition at around 470–480 nm. The spacing between them is estimated to be roughly 2000 cm^{-1}. The 0–0 and 0–1 transitions of another progression are at 449 and at ≈446 nm respectively, spacing ≈2110 cm^{-1}. The values of the spacing compare favourably with the ground-state vibrational frequency of the complexed phenylacetylide ligand and the emission of the complex has to be associated with the ligand. As expected, the emission energy is close to those

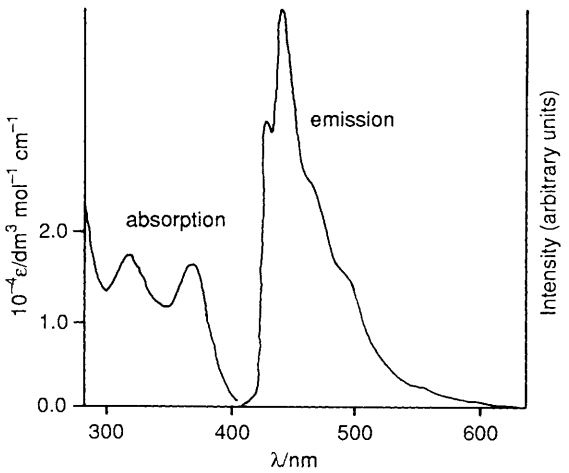

Fig. 8 Room-temperature absorption (acetonitrile) and 77 K emission [MeOH–EtOH (1:4, v/v)] spectra of $[AgPt(dppm)_2(C{\equiv}CPh)_2]PF_6$

of $[AuPt(dppm)_2(C{\equiv}CPh)_2]^+$ as well as *trans*- $[Pt(dppm)_2(C{\equiv}CPh)_2]$. The observation of two vibronic progressions with similar spacings may be due to the existence of more than one conformation of the complex in glassy solution. Different conformers may arise from the out-of-plane distortion of the silver ion. The excitation spectrum obtained with the collection wavelength set at 500 nm shows excitation bands at ≈317 and 366 nm.

Conclusion

This work has demonstrated that heterobimetallic complexes containing phenylacetylide as ligands show interesting spectroscopic and photoluminescent properties. An important aspect is the significant participation of the empty π* orbitals of the phenylacetylide in the lowest electronic excited state of the dinuclear complexes. These excited states have been found to be emissive and have long lifetimes (in the solid state). Recently we have reported spectroscopic studies and EHMO calculations on the heterobimetallic complex $[PtRh(dppm)_2(CN)_2(CNBu^t)_2]^+$.[17] The results suggested that its highest occupied molecular orbital (HOMO) is the d_{σ^*} orbital which is comprised of the valence d_{z^2} orbitals of Rh and Pt. It is therefore very interesting to investigate the spectroscopy of complexes such as $[RhPt(dppm)_2(C{\equiv}CPh)_2(CNR)_2]^+$ since one would expect to observe low-energy metal–metal bond-to-ligand charge transfer from Rh to phenylacetylide.

Acknowledgements

We acknowledge support from the Croucher Foundation, Hong Kong Research Council and National Science Council of Taiwan. H.-K. Y. is grateful for a studentship administered by the Croucher Foundation.

References

1 (*a*) L.-A. Sacksteder, E. Baralt, B. A. DeGraff, C. M. Lukehart and J. N. Demas, *Inorg. Chem.*, 1991, **30**, 2468; (*b*) E. Baralt and C. M. Lukehart, *Inorg. Chem.*, 1991, **30**, 319; (*c*) T. C. Stoner, S. J. Geib and M. D. Hopkin, *J. Am. Chem. Soc.*, 1992, **114**, 4201; (*d*) J. Manna, S. J. Geib and M. D. Hopkin, *J. Am. Chem. Soc.*, 1992, **114**, 9199.
2 H.-K. Yip, C.-M. Che and S. M. Peng, *J. Chem. Soc., Chem. Commun.*, 1991, 1626; H.-K. Yip, Ph.D. Thesis, The University of Hong Kong, 1993.
3 (*a*) C. R. Langrick, D. M. McEwan, P. G. Pringle and B. L. Shaw, *J. Chem. Soc., Dalton Trans.*, 1983, 2487; (*b*) G. R. Cooper, A. T. Hutton, C. R. Langrick, D. M. McEwan, P. G. Pringle and B. L. Shaw, *J. Chem. Soc., Dalton Trans.*, 1984, 855.
4 D. Li, H.-K. Yip, C.-M. Che, Z.-Y. Zhow, T. C. W. Mak and S.-T. Liu, *J. Chem. Soc., Dalton Trans.*, 1992, 2445.
5 J. Howell, A. Rossi, D. Wallacer, K. Haraki and R. Hoffmann, ICON, Quantum Chemistry Program Exchange, University of Indiana, 1977.
6 C. Janiak and R. Hoffman, *Inorg. Chem.*, 1989, **28**, 2743; B. E. R. Schilling and R. Hoffmann, *J. Am. Chem. Soc.*, 1979, **101**, 3456.
7 E. J. Gabe, Y. Le Page, J.-P. Charland, F. L. Lee and P. S. White, *J. Appl. Crystallogr.*, 1989, **22**, 384.
8 W. S. McDonald, P. G. Pringle and B. L. Shaw, *J. Chem. Soc., Chem. Commun.*, 1982, 861.
9 H. Masai, K. Sonogashira and H. Hagihara, *Bull. Chem. Soc. Jpn.*, 1971, **44**, 2226.
10 P. M. Gidney, R. D. Gillard and B. T. Heaton, *J. Chem. Soc., Dalton Trans.*, 1973, 132.
11 V. H. Houlding and V. M. Miskowski, *Coord. Chem. Rev.*, 1991, **111**, 145.
12 R. B. Wilson and E. I. Solomon, *J. Am. Chem. Soc.*, 1980, **102**, 4085.
13 (*a*) D. M. Roundhill, H. B. Gray and C.-M. Che, *Acc. Chem. Rev.*, 1989, **22**, 55; (*b*) S. F. Rice and H. B. Gray, *J. Am. Chem. Soc.*, 1981, **103**, 1593.
14 C.-M. Che, H.-L. Kwong, C.-K. Poon and V. W.-W. Yam, *J. Chem. Soc., Dalton Trans.*, 1990, 3215; C.-M. Che, H.-L. Kwong, V. W.-W. Yam and K.-C. Cho, *J. Chem. Soc., Chem. Commun.*, 1989, 885; C. King, J. C. Wang, N. I. Md. Khan and J. P. Fackler, jun., *Inorg. Chem.*, 1989, **28**, 2145.
15 A. L. Balch, V. J. Catalano and M. M. Olmstead, *Inorg. Chem.*, 1990, **29**, 585.
16 A. L. Balch, *J. Am. Chem. Soc.*, 1976, **98**, 8049.
17 H.-K. Yip, H.-M. Lin, Y. Wang and C.-M. Che, *Inorg. Chem.*, in the press.

Received 18*th February* 1993; *Paper* 3/00974B